To appear in proceedings of the 2005 IEEE International Conference on Intelligent Robots and Systems

Combined Optic-Flow and Stereo-Based Navigation of Urban Canyons for a UAV

Stefan Hrabar and Gaurav S. Sukhatme
Robotic Embedded Systems Laboratory
University of Southern California
Los Angeles, California, USA
{*shrabar, gaurav*}*@robotics.usc.edu*

Peter Corke, Kane Usher and Jonathan Roberts
CSIRO ICT Center
P.O. Box 883 Kenmore 4069
Queensland, Australia
{*peter.corke, kane.usher, jonathan.robers*}*@csiro.au*

***Abstract*— We present a novel vision-based technique for navigating an Unmanned Aerial Vehicle (UAV) through urban canyons. Our technique relies on both optic flow and stereo vision information. We show that the combination of stereo and optic-flow (stereo-flow) is more effective at navigating urban canyons than either technique alone. Optic flow from a pair of sideways-looking cameras is used to stay centered in a canyon and initiate turns at junctions, while stereo vision from a forward-facing stereo head is used to avoid obstacles to the front. The technique was tested in full on an autonomous tractor at CSIRO and in part on the USC autonomous helicopter. Experimental results are presented from these two robotic platforms operating in outdoor environments. We show that the autonomous tractor can navigate urban canyons using stereo-flow, and that the autonomous helicopter can turn away from obstacles to the side using optic flow. In addition, preliminary results show that a single pair of forward-facing fisheye cameras can be used for both stereo and optic flow. The center portions of the fisheye images are used for stereo, while flow is measured in the periphery of the images.**

***Index Terms*— UAV, Stereo Vision, Optic Flow, Urban Canyon Navigation.**

I. Introduction

Typically UAVs operate at high altitudes where the space around them is obstacle-free. This restriction limits the type and resolution of information that can be gathered from the onboard sensors, and thus the type of applications they can be used for. For applications such urban search and rescue, a UAV must fly at low altitudes among buildings. This means it must be able to detect obstacles around it in 3D-space, both in front and to the sides. Detecting obstacles to the side would allow the UAV to fly down the middle of a street for example, while detecting obstacles to the front would enable collision avoidance.

For ground-based mobile robots, basic obstacle avoidance is practically a 'solved problem', but for flying robots many challenges still remain. The problem is greater because these robots operate in 3D-space as apposed to the 2D plane that ground robots navigate on. Since small to medium scale UAVs have limited payload capabilities, they are unable to carry the types of sensors that are typically used for obstacle avoidance on ground-based robots (such as laser range-finders). Computer vision provides a viable sensing solution for UAVs as cameras are light and power efficient. Also, unlike a scanning type sensor, cameras take an almost instantaneous snapshot of the environment, which is beneficial on a dynamic platform.

Numerous vision-based techniques have been used for obstacle avoidance, including optic flow and stereo vision. Optic flow has been used to navigate both ground-base robots [1] [2] [3] [4] and aerial robots [5] [6] [7]. It has also been shown that bees use optic flow to avoid obstacles in flight [8]. Stereo vision has been successfully used on ground-based robots for obstacle avoidance [9] [10] [11] [12].

When navigating an urban environment, a UAV would have to deal with canyons that have 90-degree bends, T-junctions and dead-ends. This would require avoiding obstacles to the side (to keep it in the middle of a street for example), and obstacles to the front. Since optic flow is well suited to keeping a UAV equidistant from the walls of an urban canyon, and stereo vision is well suited to avoiding obstacles to the front, it seems logical to combine the two techniques for vision-based urban canyon navigation.

To determine if the combined optic flow and stereo-based approach (stereo-flow) is more effective than either of the two approaches alone, the CSIRO Autonomous Tractor was tasked to navigate an urban canyon (including 90-degree bends and T-junctions) using each of the three methods. It was able to navigate parts of the canyon using stereo or optic flow alone, but when these two techniques were combined it was able to navigate all parts. In addition to the ground-based tests, the USC autonomous helicopter (AVATAR) was controlled using optic flow, which allowed it to turn away from obstacles to the side.

Although stereo-flow combines two different vision-based techniques, these techniques do not necessarily need to operate on two different image sets. Traditionally, a pair of sideways-looking cameras would be used for optic flow, and a forward-facing pair would be used for stereo. By using a pair of forward-facing fisheye cameras, a single image pair can be used for both stereo and optic flow. The central portions of the images can be used for stereo, while the periphery can

be used for optic flow. Preliminary results for this techniques are presented: the CSIRO Autonomous Tractor is shown to have navigated a straight urban canyon using optic flow from the periphery of forward facing fisheye cameras. Also, a stereo disparity image generated from the cameras shows the feasibility of this approach

A similar approach is described in [3] where the peripheral portions of a wide-field-of-view image where used to avoid obstacles to the side, but instead of using stereo to avoid obstacles to the front, divergence-of-flow in the central portion of the image was used. Divergence-of-flow can be used to estimate the approximate time-to-contact with an obstacle that the robot is approaching. One disadvantage with this method is that the robot must be moving towards an obstacle in order to detect it.

The remainder of this paper is organized as follows: Section II discusses the use of optic flow for canyon navigation, Section III discusses stereo vision for detecting obstacles, and Section IV discusses the combination of optic flow and stereo. Section V describes the different approaches used to control the autonomous helicopter and tractor platforms. The ground and aerial-based experiments are discussed in Section VI, and the environments for these experiments are discussed in Section VII. Experimental results are presented in Section VIII, and observations are given in Section IX. Section X presents the idea of using a single pair of fisheye cameras for both optic flow and stereo, and conclusions are drawn in Section XI.

II. Optic Flow-Based Control

Optic flow is the apparent motion of features in the field of view of a moving observer. This flow can be created by two kinds of observer motion: translational ($Flow_{tr}$) and rotational ($Flow_{rot}$). [7] shows that the optic flow (F) experienced by an observer moving with translational velocity *v* and angular velocity ω while viewing an object at distance *d* and offset θ from the direction of travel can be expressed as follows:

$$F = -\omega + (v/d)\sin(\theta) \tag{1}$$

The right hand term represents flow resulting from translational motion of the observer, while the left had term represents flow from rotational motion. This relationship is illustrated in Figure 1.

As shown in Equation 1 when the observer has zero angular velocity, the flow magnitude is proportional to the translational velocity and feature angular offset, and inversely proportional to the feature distance. Closer features produce larger flows and maximum flow is generated by features perpendicular to the direction of motion (θ = 90). By solving equation 1 for *d*, we see that for a given velocity *v*, the relative distance to features can be determined from their measured flow magnitudes and angular offsets (Equation 2).

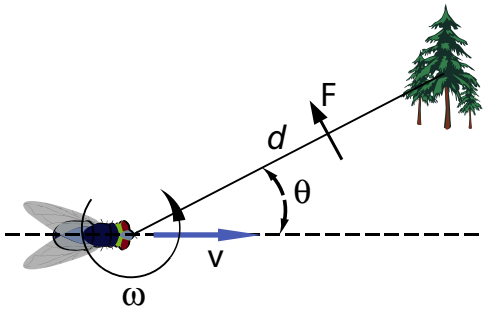

Fig. 1. Plan view of an observer moving with velocity *v* past an obstacle

$$d \propto \sin(\theta)/(F + \omega) \tag{2}$$

When the observer experiences a simultaneous translational and rotational motion (for example when travelling on a curved path), the flows due to the two types of motion are combined ($Flow_{tr}$ + $Flow_{rot}$). If we are to use the relationship in Equation 2 to measure feature distance, we need to determine ω. This can be measured with a gyroscope coupled to the cameras. Alternatively, total flow measured in portions of the image near θ = 0 can be used to approximate ω [4]. For $\theta \approx 0$, the right hand term of Equation 1 falls away meaning the flow measured is due to rotational motion alone (ω = - F).

Our approach to the problem of flow from combined translational and rotational motion has biological inspirations. [14] shows that blowflies try to minimize the time that their eyes experience a simultaneous translational and rotational motion by flying straight paths connected by brief correctional saccades. They also turn their heads very quickly to face the new direction and then turn their thorax into position. We mimic the first approach on the helicopter by flying straight while flow is recorded for a number of frames, and then stop to turn in place before continuing. Flow is not recorded while the helicopter is turning. A detailed description of how we measure flow and generate an appropriate control command can be found in [5]. In short, a command is generated which turns the the helicopter away from the side of greatest flow (closest features).

The blowfly type motion is clearly not possible with the autonomous tractor described in Section VI-A as it cannot turn in place. The tractor's limited turning angle does however mean that ω is always small and so $Flow_{rot}$ is negligible and can be ignored. Flow is therefore recorded continuously on the tractor and the steering angle adjusted in an attempt to balance the flows.

As explained in [5], wide field of view (FOV) lenses are well suited to measuring optic flow on holonomic vehicles such as helicopters. Since flow is strongest in areas perpendicular to the camera motion (θ = 90 and 270) it is best to have the cameras facing these directions. When

using standard lenses, the cameras would need to be panned to achieve this as the direction of motion changes. When using the panoramic image from a wide FOV lens, different portions of image can simply be used depending on the direction of travel. This virtual panning is far simpler to implement than physically panning a pair of cameras. The images in Fig. 2 are taken from two sideways-looking fisheye cameras during forward motion. The rectangles outline the image portions used to measure flow. Since features in the left image were closer they produced larger flow vectors.

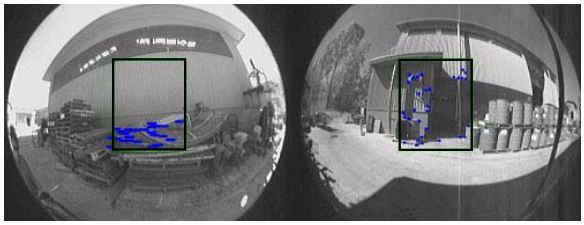

Fig. 2. Optic flow in images from sideways-facing fisheye cameras

III. Stereo Based Control

Traditionally when stereo is used for obstacle avoidance on ground-based robots, a distinction is made between the ground plane and obstacles above the ground plane that need to be avoided [15]. Cameras are usually tilted downwards so that the ground in front of the robot is visible. If the ground plane is incorrectly detected, the ground itself could be seen as an obstacle (for example when approaching an incline). Since the technique discussed in this paper is intended for use on a UAV, the ground plane assumption is not used. A flying vehicle is usually a reasonable distance above ground, and so if anything is detected in front of it, it is assumed to be an obstacle and not the ground. For the ground-based experimental runs discussed in section VI-A, the cameras where pointed straight ahead, and it was assumed that all obstacles would be tall enough to be detected by this configuration.

The Small Vision System (SVS) stereo engine from SRI [16] is used to produce 3D data from the stereo image pairs. SVS is also used for camera calibration and image rectification. Obstacle detection is performed as follows: For each frame, a turning distance threshold is applied to the 3D stereo data. All points within the threshold are projected to a 2D image, and region growing is applied to this image. A size threshold is applied to the regions to filter out noise. Each resulting region represents a feature that is within the turning distance threshold. The largest such feature is selected and a control decision is made based on its distance from the camera and position in the image. If the object is within a second distance threshold (stopping threshold), a 'Stop' command is issued. The helicopter turns in place and the tractor performs a reverse maneuver as described in section V. If the feature is outside the stopping threshold, a 'Turn' command is issued which turns the robot away from the obstacle while it moves forward. This process is illustrated in the left hand flow-diagram of Figure 4. Figs 3a, b and c show three stages in this process. Fig. 3a shows the left stereo image, b shows the disparity image, and c shows the 2D projection of the 3D data after distance thresholding and region growing. All gray areas in the image represent features within the turning threshold (3.5m in this case). The drum in the foreground has been detected as the largest and closest feature. Since it is in the left hand side of the image and is within the turning threshold but not the stopping threshold, a 'turn right' signal would be issued for this frame.

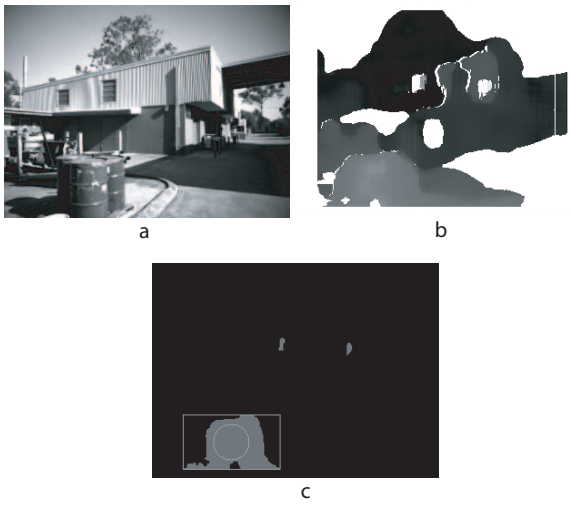

Fig. 3. Three phases in obstacle detection using stereo: a)Left image from stereo pair, b)Disparity Image, c)Obstacles detected within the turning threshold

IV. Combined Stereo and Optic Flow Based-Control

The output of the optic flow and stereo processes are combined in a hierarchical manner. Since collisions with obstacles in front of the tractor or UAV are more likely than with obstacles to the side, output from the stereo process takes precedence over that of the optic flow process. Both the stereo and optic flow processes run continuously in parallel, each producing a turn rate command. One of these commands is used as the final control output depending on whether an obstacle has been detected by the stereo process. If an obstacle is detected, the stereo process command is used, otherwise the command from the optic flow process is used for control. In subsumption architecture terms, the stereo process subsumes the optic flow process. Figure 4 illustrates these two processes and how their outputs are selected.

V. Helicopter Control vs Tractor Control

This paper describes how stereo-flow can be used to control two robotic platforms which have very different dynamics. The helicopter has six degrees of freedom, and

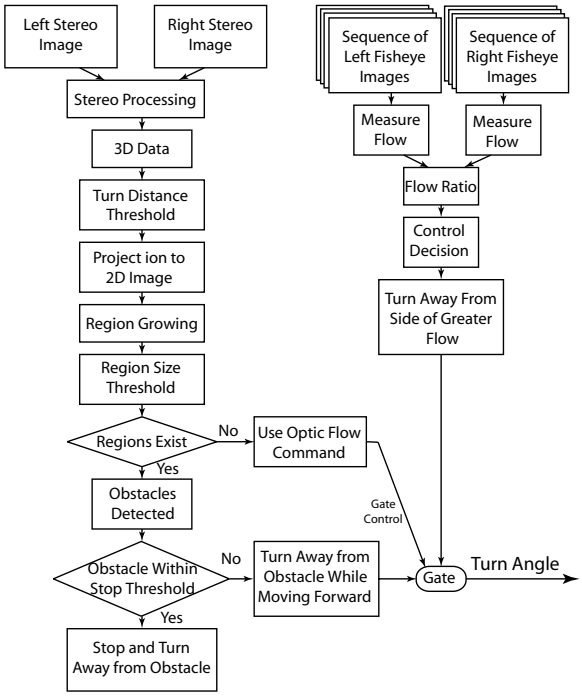

Fig. 4. Turn rate determined from Stereo and Optic Flow

can be controlled on each of these (it is holonomic), while the tractor can only be controlled in two of its three degrees of freedom. The output from the stereo-flow process therefor has to be adapted slightly, depending on the platform it is used to control. In both cases, translational motion is commanded in terms of a forward velocity. For rotation, the helicopter is given a yaw angle, while the tractor is given a steering angle. When an obstacle is detected by stereo which is within the stopping threshold, the helicopter is commanded to stop and turn in place before proceeding. Since this is not possible with the tractor, it is given a 'stop, reverse and turn' commanded. While reversing, it turns away from the obstacle. After reversing a short distance it is ready to proceed unless the obstacle is still detected. In this case it will repeat the reverse procedure until it is clear of the obstacle.

VI. Experimental Setup

A. Ground-Based Robot

For the ground-based experiments, an autonomous tractor developed at CSIRO was used [17] [18]. The vehicle (shown in Fig. 5) is a ride-on mower which has been retro-fitted with an array of actuators, sensors, and a computer system enabling the implementation and testing of control and navigation algorithms. The tractor was fitted with a forward-facing 90mm baseline stereo head from Videre Design (STH-MDCS-C), and two sideways-looking cameras fitted with 190 degree FOV fisheye lenses from OmniTech Robotics. The cameras were mounted approximately 170cm above ground level.

Fig. 5. CSIRO Autonomous Tractor

B. Aerial Robot

For the UAV-based experiments, the USC Autonomous Helicopter (AVATAR) was used [19]. The helicopter (shown in Fig. 6) is capable of autonomous flight using it's onboard sensor suite and PC-104 computer. It also carries a second computer connected to 4 FireWire cameras which is used for running vision code. Two cameras face forward as a stereo pair while the other two face sideways and are fitted with fisheye lenses. The fisheye cameras are used for optic flow-based control.

Fig. 6. USC Autonomous Helicopter platform (AVATAR)

VII. Testing Environment

A. Ground-Based Tests

The aim of the ground-based tests was to establish if it is beneficial to use a combination of optic flow and stereo based sensing for navigating urban canyons. In order to establish this, 3 typical urban canyon settings were used, namely a straight canyon, a canyon with a 90-degree bend (L-junction), and a canyon with a T-junction. Fig. 7 shows the autonomous tractor in a canyon with an L-junction at the far end.

Fig. 7. CSIRO Autonomous Tractor in a canyon with an L-junction at the end

For each type of setting, the autonomous tractor was tasked to navigate the canyon using optic flow only, stereo only, and stereo-flow. Up to five runs were performed for each of the various sensing and canyon combinations, giving a total of 33 test runs. As seen in Figs 9, 10 and 11, the canyon sections were between 5.5 and 8m wide, and up to 25m long. The average speed of the tractor during the runs was 0.5m/s. During the experiments, the velocity and steering angle of the tractor were recorded. By performing integration on this data and using a kinematic model of the tractor, its path was reconstructed to give ground truth. The tractor was oriented towards one of the canyon walls at the start so that it could not navigate the canyon by simply driving straight.

B. UAV-Based Tests

The aim of the UAV-based test was to establish if optic flow could be used to steer a UAV away from the walls of a canyon. To this end, the USC AVATAR was flown autonomously along-side obstacles at two different locations. The first was at an open field lined by tall trees on one side, while the second was at an Urban Search and Rescue training site (shown in Fig. 8). The helicopter was set off on a path parallel to the row of trees at the first site to see if the resultant flow would turn it away from the trees. At the second site it was flown between a tall tower and a railway carriage to see if it could navigate this 'canyon' by balancing the flows.

VIII. Results

A. Ground-Based Tests

The results of the ground-based test are shown in Figs 9, 10 and 11. The figures show the path taken by the autonomous tractor for each run, and the position of the canyon walls.

Table I summarizes the proportion of successful runs for each type of canyon and vision-based navigation technique. A run was deemed successful if the tractor did not collide with a canyon wall. The ratios in the table indicate the number of successful runs/number of runs attempted. "NA" indicates that no runs were attempted.

Fig. 8. USC AVATAR flying between two obstacles at the Del Valle Urban Search and Rescue Training Site

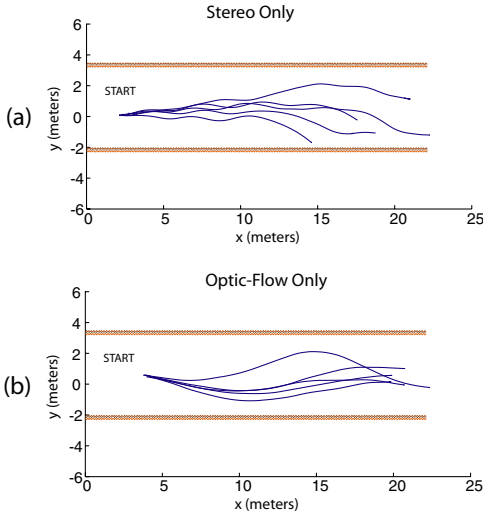

Fig. 9. Tractor paths from navigating a straight canyon using a) Stereo only, b) Optic flow only

B. UAV-Based Tests

The results of one of the UAV-based test are shown in Fig. 12. The figure shows the helicopter's path as it flew alongside a row of trees and then turned to the right after detecting the trees using optic flow. When flying at the Urban Search and Rescue Site, the helicopter was able to fly between the tower and railway carriage. As it approached the tower the flow imbalance caused it to turn towards the railway carriage, and as it approached the carriage it turned back towards the tower.

IX. Discussion of Results

For the ground-based tests, it was noted that when navigating a straight canyon using only optic flow, the tractor

TABLE I
Results For Various Control Types

Canyon Type	Flow Only	Stereo Only	Stereo-Flow
Straight	5/5	2/5	NA
L-Junction	0/3	2/5	5/5
T-Junction	NA	5/5	5/5

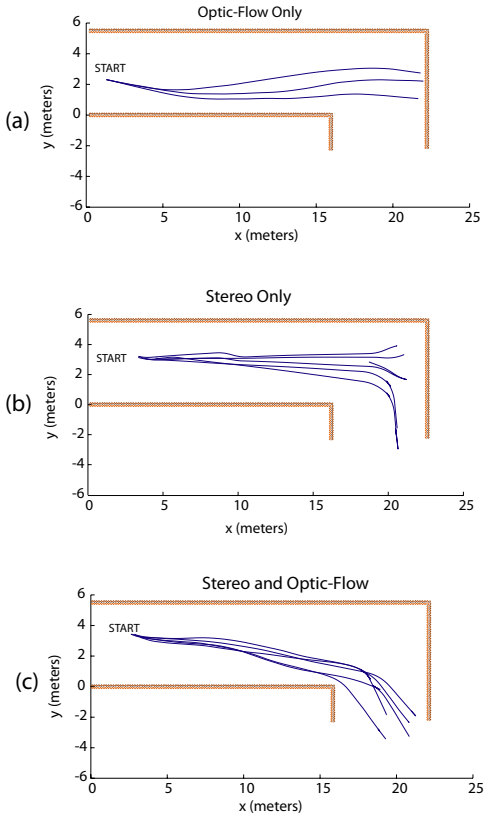

Fig. 10. Tractor paths from navigating an L-junction using a) Stereo only, b) Optic flow only, c) Optic flow and stereo

followed a relatively smooth path and was guided towards the center of the canyon. When using only stereo, the tractor followed a zigzag path, as the vehicle would have to be turned towards the canyon wall before detecting it, and would then 'bounce' off the wall and cross over the center of the canyon until it detected the opposite wall. This difference in path type (smooth vs zigzag) can be seen by comparing Figs 9 a and b.

When navigating a canyon with a 90-degree turn using only optic flow, the tractor would start to turn at the L-junction, but not sharply enough, and would eventually collide with the far wall (Fig. 10a). When using only stereo, the far wall would be detected and the tractor would turn away from it, but not always in the right direction (Fig. 10b). In some cases it would turn left and become trapped in the corner.

When using combined optic flow and stereo, the tractor successfully navigated the L-junction 5/5 times (Fig. 10c). It did not become trapped in the corner because as it entered the junction a flow imbalance would initiate a right turn. This lead to the tractor approaching the far wall obliquely so that is was detected in the left half of the stereo image. This

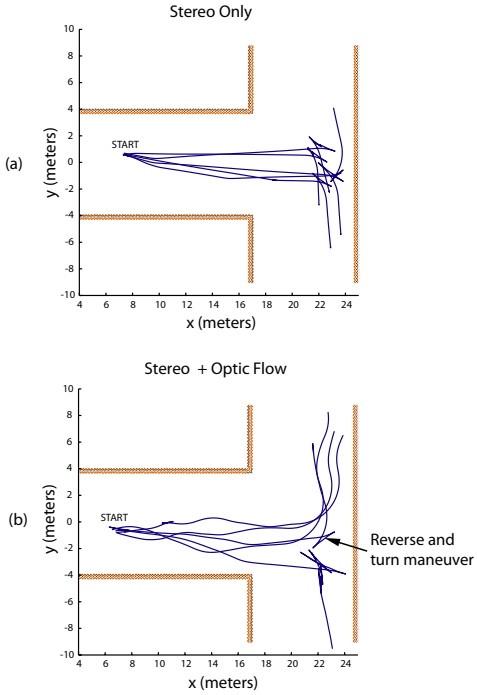

Fig. 11. Tractor paths from navigating a T-junction using a) Stereo only, b) Optic flow and stereo

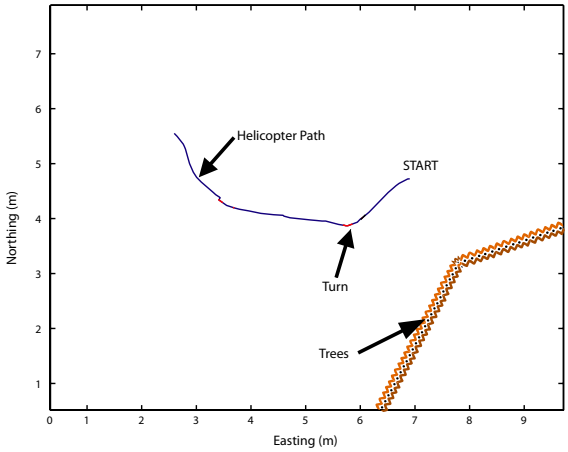

Fig. 12. Path of the helicopter as it avoided an obstacle to the left

would cause a sharp right turn allowing the tractor to exit the junction. This phenomenon is illustrated in Figure 13. At Point a the tractor has entered the junction so a canyon wall is still visible in the left fisheye image but not the right image. Flow is greater in the left image so the tractor turns right. At Point b the far wall of the canyon is detected in the stereo image. Because the flow imbalance initiated a right turn, the wall is approached obliquely from the left. The stereo-based avoidance detects the wall to the left and commands a sharp right turn.

The results for a T-junction were similar to that of the L-junction. Using optic flow only, the far wall of the junction

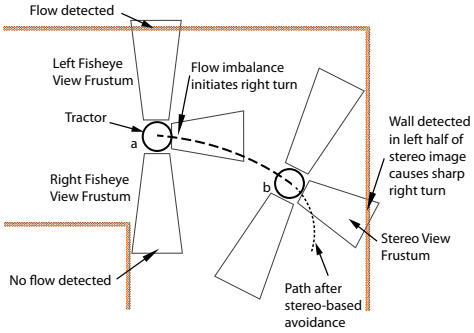

Fig. 13. A flow imbalance initiates a turn away from the junction corner

would not be detected, leading to a collision. Using stereo only, the far wall would be detected, and the tractor would then either turn left or right to avoid the wall, depending on its orientation as it entered the junction (Fig. 11a). Unlike for the L-junction though, it did not matter which way the tractor turned as there were no corners to trap it. Combined optic flow and stereo produced a 5/5 success rate once again for this type of junction, showing it is a suitable combination for navigating T-junctions (Fig. 11b). Both Figures 11a and b show evidence of the tractor performing 'reverse and turn' maneuvers when the far wall is detected by stereo. As described in Section V, this occurs when an obstacle is detected within the stopping threshold.

When flying the helicopter alongside a row of trees, the optic flow-based control was able to turn it away from the trees successfully 5/8 times. Although it failed to turn away from the trees on occasion, it never turned towards the trees. A single successful flight was made between the tower and railway carriage. The other flights were aborted as the helicopter was blown dangerously close to the obstacles.

X. Stereo and optic flow From a Single Pair of Fisheye Cameras

As shown by the results mentioned in section VIII-A, the combination of stereo and optic flow-based navigation is effective in urban canyon environments. One drawback with this combination is the need for 4 cameras. An alternative solution is to use the images from a single pair of forward-facing fisheye cameras for both stereo and optic flow. Since the lenses have 190 degree FOV's, even when they are pointed forward the walls of an urban canyon are still visible in the peripheral portion of the images. Flow information can be measured from these portions of the image and used for the centering response.

Since both cameras are pointed forward, they can also be used as a stereo pair. Instead of attempting to perform stereo on the full fisheye image, a central region of each image can be extracted. At the center of a fisheye image, the lens distortion is smallest, and so this portion of the image is similar to that produced by a standard lens. Fig. 14 shows the images from a pair of forward-facing fisheye cameras. The rectangles on the outer edges of the images represent the areas in which flow is measured. The central rectangles represent the portion of the images that are used for stereo. Figs 15a, b and c illustrate three stages of obtaining 3D data from the fisheye lenses. Fig. 15a is the central portion of the fisheye image after rectification, b is the disparity image, and c is a 3D reconstruction of the scene.

Fig. 14. Images from a par of forward-facing fisheye cameras

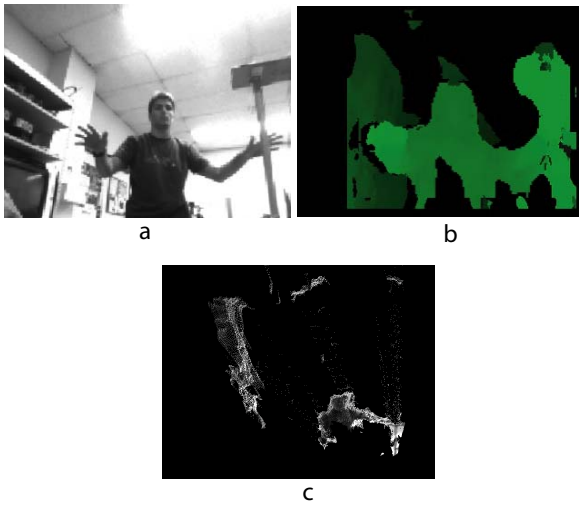

Fig. 15. Stereo from fisheye cameras: a) Central portion of the fisheye image after rectification, b) Disparity image, c) 3D data

Although the canyon walls are visible in the peripheral portions of the fisheye images, these portions are also highly distorted making it difficult to measure flow here. To test if these portions of the image could be used for flow-based control, the CSIRO Autonomous Tractor was fitted with a pair of forward-facing fisheye cameras and tasked to navigate a straight urban canyon using only optic flow. Fig. 16 shows the tractor's path for these runs, and as can be seen, It successfully navigated the canyon 4/5 times.

Although stereo data from the fisheye images has not yet been used for control, initial tests seem promising. As can be seen in Figure 15, the disparity image obtained is a reasonable representation of the scene. A drawback with using wide angle lenses for stereo is the reduced resolution of the images which reduces the range resolution. The results shown in Fig. 15 are from 320x240 images. By performing

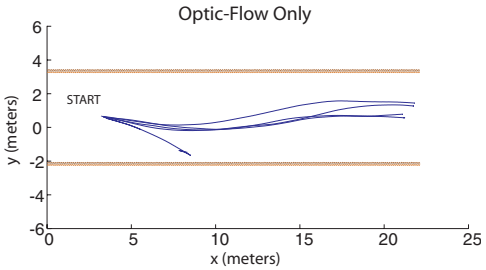

Fig. 16. Tractor paths from navigating a straight canyon using only optic flow from a pair of forward facing fisheye cameras

stereo on full-frame (640x480) images, it is hoped that features up to 5m away well be detected. Although this is a fairly short sensor range, it may be sufficient for navigating urban canyons with an autonomous helicopter, as a helicopter can travel slowly and stop in place when an obstacle is detected, unlike a fixed-wing UAV.

XI. Conclusions and Future Work

The experimental results show that combined stereo and optic flow based control can be used to navigate a ground-based robot through urban canyons with various types of junctions. Also, optic flow based control can be used to steer a UAV away from obstacles to the side. While using optic flow based control alone can keep a robot near the center of an urban canyon, it cannot be used to negotiate T- and L-junctions. Using stereo only, a straight canyon can be navigated, but this results in the robot following a zigzag path and can lead to it being trapped in corners. By combining stereo and optic flow based control, the strengths of each of these types of control can be used to produce a system that is more reliable at navigating urban canyons than either system on its own. Preliminary results show that a UAV could potentially be controlled using optic flow and stereo information from a single pair of forward-facing fisheye cameras. In the future we hope to test combined stereo and optic flow-based control of the USC Autonomous Helicopter, either using two pairs of cameras or a single pair of forward-facing fisheye cameras.

Acknowledgments

This work is supported in part by DARPA under grants DABT63-99-1-0015 and 5-39509-A (via UPenn) as part of the Mobile Autonomous Robot Software (MARS) program. The authors would like to thank the following group of people from the CSIRO ICT Center who played an integral role in the ground-based work: Graeme Winstanley, Leslie Overs, Stephen Brosnan and Craig Worthington. Also, Alan Butler who acted as the safety pilot for the UAV-based work, and Lawrence Collins from the Urban Search and Rescue Task Force of the Los Angeles Fire Department for making the Del Valle site available for flight tests.

References

[1] Ben Krse, Anuj Dev, Xaro Benavent, and Frans Groen, "Vehicle navigation on optic flow," .

[2] A.N.U. Biorobotic Vision Laboratory Homepage, "http://cvs.anu.edu.au/bioroboticvision/rslide1.html," .

[3] Ted Camus, David Coombs, Martin Herman, and Tsai-Hong Hong, "Real-time single-workstation obstacle avoidance using only wide-field flow divergence," *Videre: Journal of Computer Vision Research*, vol. 1, no. 3, pp. 30–57, 1999.

[4] Antonis A. Argyros, Dimitri P. Tsakaris, and Cédric Groyer, "Bio-mimetic centering behavior for mobile robots with panoramic sensors," *IEEE Robotics and Automation Magazine*, vol. 11, no. 4, pp. 21–68, 2004.

[5] Stefan E. Hrabar and Gaurav S. Sukhatme, "A comparison of two camera configurations for optic-flow based navigation of a uav through urban canyons," in *IEEE/RSJ International Conference on Intelligent Robots and Systems*, 2004.

[6] Laurent Muratet, Stephanie Doncieux, and Jean-Arcady Meyer, "A biometric navigation system using optical flow for a rotary-wing uav in urban environment," in *ISR2004*, March 2004.

[7] W.E. Green, P.Y. Oh, and G.L. Barrows, "Flying insect inspired vision for autonomous aerial robot maneuvers in near-earth environments," in *Proceedings of the 2004 IEEE International Conference on Robotics and Automation*, New Orleans, LA, April.

[8] MV Srinivasan, M Lehrer, WH Kirchner, and SW Zhang, "Range perception through apparent image speed in freely flying honeybees," in *Vis Neurosci. 1991 May;6(5):519-35*.

[9] Steven B. Goldberg, Mark W. Maimone, and Larry Matthies, "Stereo vision and rover navigation software for planetary exploration," in *Proceedings of the IEEE IEEE Aerospace Conference*, Big Sky, Montana, USA, March 2002.

[10] S. Badal, S. Ravela, B. Draper, and A. Hanson, "A practical obstacle detection and avoidance system," in *WACV94*, 1994, pp. 97–104.

[11] L. Iocchi and K. Konolige, "A multiresolution stereo vision system for mobile robots," 1998.

[12] S. Singh and B. Digney, "Autonomous cross-country navigation using stereo vision," 1999.

[13] G.L. Barrows, J.S. Chahl, and M.V. Srinivasan, "Biomimetic visual sensing and flight control," in *Bristol UAV Conference*, Bristol, UK, April.

[14] C. Schilstra and J.H. van Hateren, "Blowfly flight and optic flow. i. thorax kinematics and flight dynamics," in *J.Exp.Biol. 202:1481-1490, 1999*.

[15] Darius Burschka, Stephen Lee, and Gregory Hager, "Stereo-based obstacle avoidance in indoor environments with active sensor re-calibration," in *Proceedings of the IEEE International Conference on Robotics and Automation (ICRA2001)*, Washington, DC, May 2002.

[16] SRI Stereo Engine Homepage, "http://www.ai.sri.com/ konolige/svs/," .

[17] Kane Usher, Matthew Dunbabin, Peter Corke, and Peter Ridley, "Robust pose estimation for a car-like vehicle," in *Proceedings of the International Conference on Robotics and Automation*, New Orleans, USA, 2004, pp. 5129–5134, IEEE.

[18] K. Usher, P. Ridley, and P.I. Corke, "Visual servoing of a car-like vehicle - an application of omnidirectional vision," Taipei, Sept. 2003, pp. 4288–429.

[19] USC Autonomous Flying Vehicle Homepage, "http://www-robotics.usc.edu/˜avatar," .